) Cyclic peptides: J. M. McDonnell, D. Fushman, S. M. Cahill, B. J. Sutton, D. Cowburn, *J. Am. Chem. Soc.* **1997**, *119*, 5321; M. Favre, K. Moehle, L. Jiang, B. Pfeiffer, J. A. Robinson, *J. Am. Chem. Soc.* **1999**, *121*, 2679.

[9] Peptides **2**–**4** were synthesized by solid-phase methods and purified by reverse-phase HPLC. The structures were confirmed by matrix-assisted laser desorption/time of flight mass spectrometry (MALDI-TOF MS) and by high-resolution ^{1}H NMR spectroscopy.

[10] a) T. S. Haque, J. C. Little, S. H. Gellman, *J. Am. Chem. Soc.* **1994**, *116*, 4105; b) S. Awasthi, S. Raghothama, P. Balaram, *Biochem. Biophys. Res. Commun.* **1995**, *216*, 375; c) T. S. Haque, J. C. Little, S. H. Gellman, *J. Am. Chem. Soc.* **1996**, *118*, 6975; d) I. L. Karle, S. K. Awasthi, P. Balaram, *Proc. Natl. Acad. Sci. USA* **1996**, *93*, 8189; e) H. L. Schenck, S. H. Gellman, *J. Am. Chem. Soc.* **1998**, *120*, 4869; f) C. Das, S. Raghothama, P. Balaram, *J. Am. Chem. Soc.* **1998**, *120*, 5812; g) S. R. Raghothama, S. K. Awasthi, P. Balaram, *J. Chem. Soc. Perkin Trans. 2* **1998**, 137; h) C. Das, S. Raghothama, P. Balaram, *Chem. Commun.* **1999**, 967.

[11] P. Guntert, C. Mumenthaler, K. Wüthrich, *J. Mol. Biol.* **1997**, *273*, 283.

[12] K. Wüthrich, *NMR of Proteins and Nucleic Acids*, Wiley, New York, **1986**.

[13] Use of $H_\alpha - H_\alpha$ NOE interactions to determine β-hairpin population: a) Ref. [8b]; b) Ref. [8c]; c) E. de Alba, J. Rico, M. A. Jiménez, *Protein Sci.* **1997**, *6*, 2548; d) M. Ramírez-Alvarado, F. J. Blanco, H. Niemann, L. Serrano, *J. Mol. Biol.* **1997**, *273*, 898.

[14] F. A. Syud, J. F. Espinosa, S. H. Gellman, *J. Am. Chem. Soc.* **1999**, *121*, 11577.

[15] a) D. S. Wishart, B. D. Sykes, F. M. Richards, *J. Mol. Biol.* **1991**, *222*, 311; b) D. S. Wishart, B. D. Sykes, F. M. Richards, *Biochemistry* **1992**, *31*, 1647.

[16] We have recently shown that a cyclic 14-residue peptide containing two D-Pro–Gly loop segments, similar to **4**, displays very high population of the β-sheet conformation in aqueous solution (Ref. [14]); analogous behavior was observed for **4** (manuscript in preparation).

[17] The β-hairpin population of **2** was estimated at each indicator residue and temperature by interpolating the $\delta_{H\alpha}$ value for **2** between the $\delta_{H\alpha}$ value for the corresponding residue in unfolded reference **3** at that temperature and the $\delta_{H\alpha}$ value for folded reference **4** at 276 K. (We assume that **4** is maximally folded at low temperature.)

[18] Attempted population analysis based on $\delta_{H\alpha}$ data for the non-hydrogen-bonded strand residues of **2** (Trp 2, Tyr 4, Phe 9, and Val 11) and reference peptides **3** and **4** provides nonsensical results. For example, at 275 K, $\delta_{H\alpha}$ data for Trp 2 imply 180 % β-hairpin population for **2**, while $\delta_{H\alpha}$ data for Phe 9 imply < 0 % β-hairpin population for **2**. We suspect that subtle differences in aromatic sidechain packing between cyclic peptide **4** and the fully folded state of **3** are responsible for these observations. (This hypothesis requires differences of < 0.3 ppm in non-hydrogen-bonded residue $\delta_{H\alpha}$ values between these two systems.) Although **4** appears not to be a fully accurate model for interstrand sidechain packing in the β-hairpin conformation of **3**, we believe that **4** is a good model for the backbone in the β-hairpin conformation of **3** because of the good agreement among data for the four hydrogen-bonded strand residues (Gln 3, Val 5, Lys 8, and Thr 10) and for the Gly residue in the turn (see Ref. [19]).

[19] The folding equilibrium of a designed β-hairpin has been monitored by the chemical shift separation ($\Delta\delta_{H\alpha}$) between the geminal α-protons of a glycine residue in the loop (loop sequence = Asn–Gly): M. S. Searle, S. R. Griffiths-Jones, H. Skinner-Smith, *J. Am. Chem. Soc.* **1999**, *121*, 11615. We estimated the β-hairpin population of **2** by interpolating between $\Delta\delta_{H\alpha}$ values for reference peptides **3** and **4**. This analysis indicated 66 % β-hairpin population for **2** at 275 K, and 56 % at 315 K; these estimates agree well with those obtained from strand residue $\delta_{H\alpha}$ data.

[20] A. J. Maynard, G. J. Sharman, M. S. Searle, *J. Am. Chem. Soc.* **1998**, *120*, 1996.

[21] After this report was submitted for publication, a thermodynamic analysis of β-hairpin formation by GB1-derived peptide **1** appeared: S. Honda, N. Kobayashi, E. Munekata, *J. Mol. Biol.* **2000**, *295*, 269. These authors concluded that β-hairpin formation is enthalpically favorable ($\Delta H = -13$ kcal mol^{-1}) and entropically unfavorable ($\Delta S = -43$ e.u.) near room temperature. The signs of these thermodynamic parameters match the signs of the parameters we deduce for **2**, but the parameters for **1** are approximately fourfold larger. This quantitative difference may arise because of sequence differences between **1** and **2** and/or because Honda et al. assumed $\Delta C_p = 0$ for β-hairpin formation by **2**, which may not be correct.

[22] a) R. L. Baldwin, *Proc. Natl. Acad. Sci. USA* **1986**, *83*, 8069; b) R. S. Spolar, J. H. Ha, M. T. Record, *Proc. Natl. Acad. Sci. USA* **1989**, *86*, 8382; c) J. R. Livingstone, R. S. Spolar, M. T. Record, *Biochemistry* **1991**, *30*, 4237.

[23] a) K. A. Dill, *Biochemistry* **1990**, *29*, 7133; b) W. Blokzijl, J. B. F. N. Engberts, *Angew. Chem.* **1993**, *105*, 1610; *Angew. Chem. Int. Ed. Engl.* **1993**, *32*, 1545.

[24] Leading references on the contributions of hydrogen bonds to the stability of folded peptides and proteins: a) B. A. Shirley, P. Stanssens, U. Hahn, C. N. Pace, *Biochemistry* **1992**, *31*, 725; b) B. P. P. Huyghues-Despointes, T. M. Klinger, R. L. Baldwin, *Biochemistry* **1995**, *34*, 13267; c) M. P. Byrne, R. L. Manuel, L. G. Lowe, W. E. Stites, *Biochemistry* **1995**, *34*, 13949.

[25] β-Hairpin formation by **5** in 50 % aqueous methanol is enthalpically favorable and entropically unfavorable at 298 K, which has been interpreted to indicate that interstrand hydrogen bond formation provides an enthalpic driving force for folding in this mixed solvent (Ref. [20]).

[26] a) D. B. Smithrud, T. B. Wyman, F. Diederich, *J. Am. Chem. Soc.* **1991**, *113*, 5420; b) D. B. Smithrud, F. Diederich, *J. Am. Chem. Soc.* **1990**, *112*, 339.

[27] G. I. Makhatadze, P. L. Privalov, *Biophys. Chem.* **1994**, *50*, 285, and references therein.

Complimentary Polytopic Interactions**

Ekaterina O. Arikainen, Neville Boden, Richard J. Bushby,* Owen R. Lozman, Jeremy G. Vinter, and Andrew Wood

Substantially enhanced mesophase ranges can be obtained by mixing the discotic liquid crystal **1a** with one equivalent of the "larger core" polynuclear aromatic compounds **2a** or **3a** (Scheme 1). The special stability of these novel π-stacked systems is not the result of either charge-transfer or (net) quadrupolar interactions but instead arises from a complimentary polytopic interaction (CPI).

Chemical doping of discotic liquid crystals is well known and, in some cases, it produces enhanced mesophase ranges.[1] Hence, mixtures of the discotic liquid crystal **1a** with 2,4,7-trinitrofluoren-9-one (TNF) have been extensively studied.[2] Although charge-transfer bands are observed in the UV/Vis spectrum of this mixture, they are weak. It is now believed

[*] Prof. R. J. Bushby, E. O. Arikainen, Prof. N. Boden, O. R. Lozman, A. Wood
Centre for Self-Organising Molecular Systems (SOMS)
University of Leeds, Woodhouse Lane, Leeds LS2 9JT (UK)
Fax: (+44) 113-233-6452
E-mail: R.J.Bushby@chem.leeds.ac.uk
J. G. Vinter
The University Chemical Laboratory
Lensfield Road, Cambridge CB2 1EW (UK)

[**] Complimentary Polytopic Interactions, Part 1. This work was supported by BDH (Merck Ltd.) and the EPSRC. The photoconductivity experiment and synthesis of large-core molecules **2** and **3** are reported elsewhere.[4, 12]

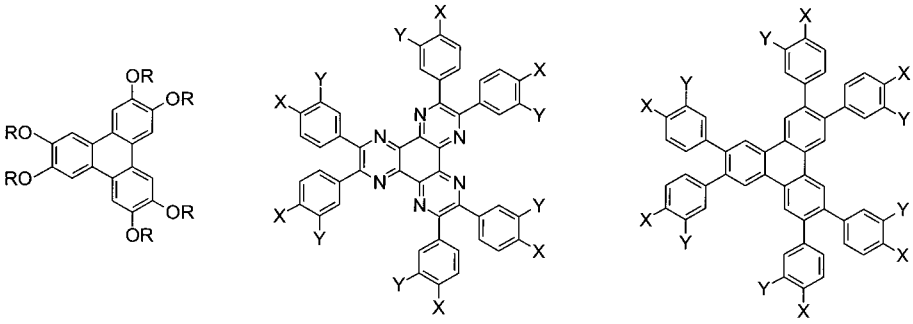

Scheme 1. Molecules used in this investigation are the small-core discogens **1** and the large-core polynuclear aromatic species **2** and **3**, which differ only by atomic (N, C) substitution.

that quadrupolar interactions between the two components produce the dominant stabilizing effect and that charge transfer is coincidental.[3] Nevertheless, almost all known examples of "chemical doping" of discotic materials have involved electron donor–electron acceptor pairs.

2,3,6,7,10,11-Hexakis(hexyloxy)triphenylene **1a** displays a hexagonal-columnar mesophase between 70 and 100 °C. When mixed with the azatriphenylene **2a** (which has itself two crystalline forms that melt at 71 °C and 81 °C) in a 1:1 ratio, a new liquid crystal **A** is formed, with a hexagonal-columnar phase between 130 °C and 240 °C. The transition at 240 °C is isothermal. The phase behavior of the components **2** and **3** and their mixtures with **1a** are shown in Table 1.[4]

Table 1. Phase transitions of the pure components and mixtures studied in this investigation.

Molecule/mixture	Phase transition T [°C] (ΔH [kJ mol^{-1}])[a]
1a	Cr 70 (48.3), Col_h 100 (7.1), I
2a	Cr 71 (34.3), Cr 81 (variable), I
2b	Cr_1 98 (32.0), Cr_2 147 (6.7), Col_1 150 (10.2), Col_r 194 (31.8), I
3a	Cr 59 (27.0), I
3b	Cr 65 (1.3), Col_h 135 (12.5), I
1a + **2a** (**A**)	Solid ≈130 (0.0), Col_h 240 (37.6), I
1a + **3a** (**B**)	Cr 66 (3.4), Col_h 155 (18.3), I

[a] The transition temperatures and enthalpies were measured by DSC (Perkin-Elmer DSC7, sample 2–3 mg in closed Al pans, heating rate +10 K min^{-1}). Phases were assigned from polarizing optical microscopy and X-ray diffraction data.

Thin-layer chromatography of **A** shows two distinct spots, corresponding to **1a** and **2a**. The UV/Vis (as a solid or a $CHCl_3$ solution), the ^{1}H NMR (as a solution in $CDCl_3$ or C_6D_6), and the IR (as a solid or nujol mull) spectra of the mixture prove to be simply a sum of those of the two components. Apparently, there is no covalent bonding between the two components and their electronic structures are not perturbed in any significant way.

The optical texture of **A** is similar to that obtained for many columnar mesophases (Figure 1). When a thin film between glass slides is annealed at 230 °C overnight, a homeotropic alignment is obtained.

The diffraction maxima in the small-angle region of the X-ray diffraction (XRD) pattern are sharper and more numerous in **A** than those of **1a**. The diffuse wide-angle maximum is typical of a columnar liquid crystal, however, the suggestion is that this phase is much more highly ordered. This is also consistent with the rather high enthalpy associated with the Col→I transition (+37.6 kJ mol^{-1} for **A**, a ½ : ½ molar mixture of **1a**:**2a**, compared to +7.1 kJ mol^{-1} for **1a**). The unit cell parameters

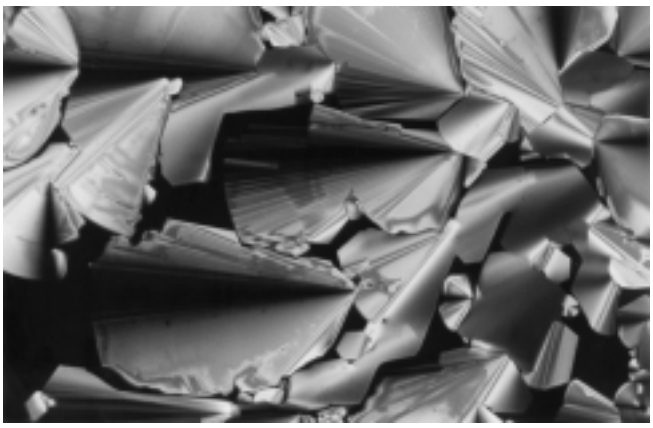

Figure 1. Optical texture of **A** as it appears when viewed through cross-polarizing filters at 240 °C (×100).

for this and the related mixture, **B** (**1a** + **3a**), are given in Table 2.

The fact that there is a single column/column repeat distance C and a hexagonal lattice shows that there cannot be segregated stacks of **1a** and **2a**. There is probably an alternating structure of the type shown in Figure 2.

Over most of the composition range, **A** is immiscible with both **1a** and **2a** (Figure 3). Along with the enhanced phase behavior and changes in ordering, this confirms that there is a very strong interaction between **1a** and **2a**.

Table 2. Calculated cell parameters from XRD measurements[a] on some of the pure components and their mixtures.

Molecule/mixture	a_{hex} [Å]	C [Å]	Number of reflections
1a	24.2	3.55	3
2a	30.5	3.55	7
3a	29.6	3.55	7
1a + **2a** (**A**)	28.3	6.92[b]	11
1a + **3a** (**B**)	27.0	7.07[c]	15

[a] Diffraction patterns were collected on film using a pinhole camera consisting of a Philips generator and tubes, Ni-filtered $Cu_{K\alpha}$ radiation (λ = 0.154 nm), and a Lindemann sample tube (1.5 mm inner diameter) to a plate 135.5 mm distant. [b] Average ring separation 3.46 Å. [c] Average ring separation 3.54 Å.

  0044-8249/00/11213-2424 $ 17.50+.50/0 *Angew. Chem.* **2000**, *112*, Nr. 13

Figure 2. Representation of the probable stacking of **1a** and **2a** in **A**.

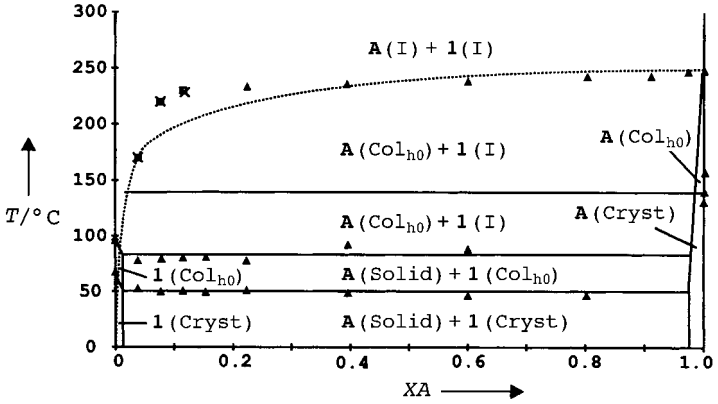

Figure 3. Phase versus composition diagram for binary mixtures of **1a** and **A** (data points are those measured by differential scanning calorimetry (DSC) and optical polarizing microscopy (OPM)). The liquidus of the phase diagram for an ideal mixture of solid **1a**:**2a** (=**A**, which dissociates completely upon melting to **1a** and **2a**) against component **1a** is given by Equation (1), where x_1 is the mole fraction of **1a**, ΔH_A is the enthalpy change at the clearing point of **A** (for a ½:½ molar ratio **1a**:**2a**), T_m is the melting point of pure **A**, and T is the melting point of the mixture (**1a** + **A**).[5].

A stable mixture, **B**, is also formed between **3a** (the carbon-atom analogue of **2a**) and **1a**. The phase diagram for mixtures of **1a** and **B** fits the same thermodynamic model as mixtures of **1a** and **A**. Once again, X-ray diffraction shows the mixture to be more highly ordered than **1a**. In contrast, no stabilized mixture is obtained when **1** is mixed with the more highly substituted molecules **2b** or **3b**.

Stable mixtures formed by the discogen **1a** with TNF have previously been modeled by treating the components as Gay–Berne disks with associated (net) quadrupole moments.[6] On this basis, we expect the molecular components of the stable 1:1 mixtures formed between the discogen **1a** and compounds **2a** and **3a** should carry opposite quadrupoles. Table 3 shows calculated values for the net quadrupoles of the aromatic cores of these molecules and it is evident from these calculations that this is not the case.

Table 3. Calculated dipole (μ) and quadrupole (Θ) moments for the pure components.

Molecule[a]	μ [D]	Θ [e A^2]	Observed[b]	Expected[c]
C_6H_6	0.00	−16.8	–	–
C_6F_6	0.00	17.9	–	–
1b	0.02	−47.1	–	–
2c	0.01	−83.4	Yes	No
2d	0.06	106.6	No	Yes
3c	0.03	−71.3	Yes	No
3d	0.08	178.2	No	Yes

[a] Benzene and hexafluorobenzene are shown as an example of a binary mixture that forms an induced phase.[7] [b] Stable mixture with **1** observed experimentally. [c] Stable mixture with **1** expected on the basis of the (net) quadrupolar model.[6]

In order to understand the nature of the interactions in these π-stacked systems properly, a dispersed, polytopic description of the molecular charge distribution is required. We have modeled these mixtures using an extended electron distribution (XED) based upon that exploited by Hunter.[8, 9] This method involves displacing nonbonded electrons (such as π electrons and lone pairs) from the atomic centers to leave a positive charge at the nucleus.[10] This effectively generates a set of quadrupole moments dispersed on each atom of the system. This provides a more realistic charge distribution than is available using traditional atom-centered charge methods or by assuming that it is the net molecular dipole or quadrupole that dominates.[10] The geometries of the molecules under investigation (**1b**, **2c**, **2d**, **3c**, **3d**) were optimized using the AM1 semiempirical routine in the MOPAC package.[11] After the extended electrons were added, a conformational search was performed. The docking routine then brought one moveable (but conformationally fixed) molecule towards an immobile (and conformationally fixed) molecule from every direction using a free SIMPLEX minimizer. In each case, where stable pairs are formed, the same minima were obtained from many of these starting configurations. The output from the docking experiment gives the overall interaction energy and its van der Waals and coulombic contributions. From this output, the minimum energy intermolecular conformations can also be visualized. By comparing the interactions between the molecules and themselves (such as **1b** + **1b** and **2c** + **2c**) and the mixed system (such as **1a** + **2c**) it is possible to predict whether or not a stable mixture will form. These figures (Table 4) agree with the experimentally observed trends in mixture formation and stability. Representations of the minimum energy "stacks" for **1b** + **1b** and **3c** + **3c** and their mixture (**1b** + **3c**) are shown in Figure 4.

Compounds **2a** and **3a** have different electronic characteristics but similar shapes. Mixtures of both **2a** and **3a** with 2,3,6,7,10,11-hexakis(alkoxy)triphenylenes of varying chain lengths **1*n*** (n = 4–16) behave in a similar manner (Figure 5). In both cases there is an optimum side-chain length for the **1*n***

Table 4. Results from the XED calculations.

Mixture[a]	Mean energy [kJ mol^{-1}]	Observed[b]	Expected[c]
$C_6H_6 + C_6H_6$	−4.7	–	–
$C_6F_6 + C_6F_6$	−5.2	–	–
$C_6H_6 + C_6F_6$	−10.6	–	–
1b + **1b**	−39.8	–	–
2c + **2c**	−37.3	–	–
2c + **1b**	−41.2	Yes	Yes
2d + **2d**	−51.6	–	–
2d + **1b**	−40.9	No	No
3c + **3c**	−36.5	–	–
3c + **1b**	−49.9	Yes	Yes
3d + **3d**	−41.0	–	–
3d + **1b**	−32.6	No	No

[a] Benzene and hexafluorobenzene are shown as an example of a binary mixture that forms an induced phase (see Table 3). [b] Stable mixture with **1** observed experimentally. [c] Stable mixture with **1** expected on the basis of the XED/CPI model.

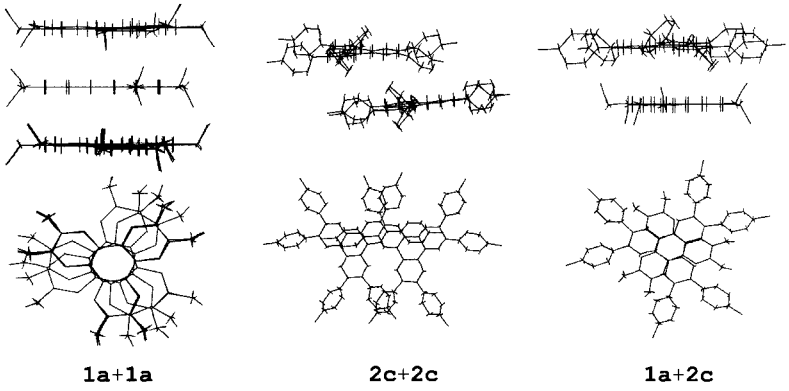

Figure 4. The elevation and plan views of the XED minimum energy dock of two molecules for a system which forms a stable mixture with **1b**. Left: **1b** + **1b**; middle: **3c** + **3c**; right: the mixture **1b** + **3c**.

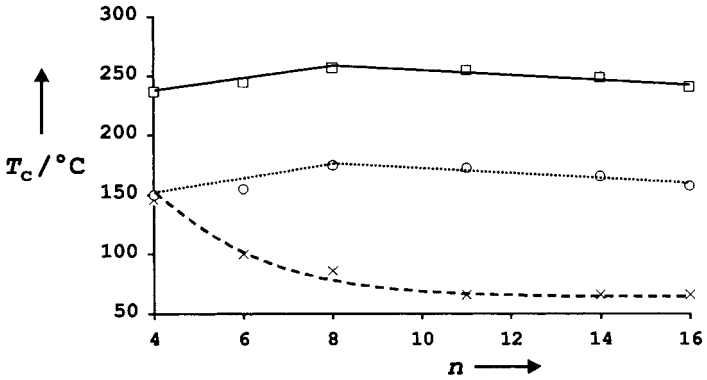

Figure 5. The trends in clearing temperature T_c for binary mixtures of the large core molecules (**2a** and **3a**) with discogen **1*n*** as a function of chain length *n*, measured by DSC and OPM. Upper line (——) = **1*n*** + **2a**; middle line (••••) = **1*n*** + **3a**; lower line (- - - -) = **1*n*** alone.

component, presumably corresponding to the same optimum packing. This stabilizing effect vanishes in those systems where the side chains are too long and no stable mixtures are obtained, or even predicted, for the systems **1a** + **2b** or **1a** + **3b** (**1b** + **2d**, **1b** + **3d**) in which the number of side-chain (x + y) is doubled to twelve. Hence, although the XED – CPI approach seems to be the only way to rationalize the stability of these mixtures, the packing of side chains is also important.

These mixtures not only provide a novel way of designing π-stacked systems but, from the standpoint of some applications, these particular systems are attractive. For example, mixtures obtained in this way are better photoconductors, with higher charge mobilities (for example, the mobility is $\sim 0.02\ cm^2 V^{-11} s^{-11}$ for **3a** + **1*n*** ($n = 11$)) than the discotic liquid crystal **1*n*** alone (**1*n*** ($n = 11$) is $3 \times 10^{-4}\ cm^2 V^{-11} s^{-11}$).[12] This enhanced mobility begins to approach the highest known values for discotic liquid crystals ($0.1\ cm^2 V^{-11} s^{-11}$).[13]

Received: December 14, 1999
Revised: April 13, 2000 [Z14395/Z14397]

[1] K. Praefcke, J. D. Holbery, *J. Inclusion Phenom. Mol. Recognit. Chem.* **1996**, *24*, 19.
[2] W. Kranig, C. Boeffel, H. W. Spiess, O. Karthaus, H. Ringsdorf, R. Wustefeld, *Liq. Cryst.* **1990**, *8*, 375.
[3] M. A. Bates, G. R. Luckhurst, *Liq. Cryst.* **1998**, *24*, 229.
[4] New synthesis of large core discogens: N. Boden, R. J. Bushby, G. Headdock, O. R. Lozman, A. Wood, *Liq. Cryst.*, submitted.
[5] H. A. J. Oonk, *Phase Theory, The Thermodynamics of Heterogeneous Equilibria, Vol. 3*, Elsevier Scientific, Amsterdam, **1981**, pp. 175 – 178.
[6] M. A. Bates, G. R. Luckhurst, *Liq. Cryst.* **1998**, *24*, 229.
[7] T. Dahl, *Acta. Chem. Scand.* **1973**, *27*, 995.
[8] C. A. Hunter, J. K. M. Saunders, *J. Am. Chem. Soc.* **1990**, *112*, 5525.
[9] C. A. Hunter, *Angew. Chem.* **1993**, *105*, 1653; *Angew. Chem. Int. Ed. Engl.* **1993**, *32*, 1584.
[10] J. G. Vinter, *J. Comput. Aided Mol. Des.* **1996**, *10*, 417.
[11] MOPAC and SIMPLEX as implemented in the COSMIC modelling system, J. G. Vinter, Cambridge, **1996**.
[12] Enhanced electronic transport properties: N. Boden, R. J. Bushby, K. J. Donovan, T. Kreouzis, O. R. Lozman, *J. Chem. Phys.*, submitted.
[13] D. Adam, P. Schuhmacher, J. Simmerer, L. Haussling, K. Siemensmeyer, K. H. Etzbach, H. Ringsdorf, D. Haarer, *Nature* **1994**, *371*, 141 – 143.

Rhodium – Rhodium Bonds in Edge-Sharing Coplanar Dinuclear Complexes**

Cristina Tejel, Milena Sommovigo, Miguel A. Ciriano,* José A. López, Fernando J. Lahoz, and Luis A. Oro*

Dinuclear rhodium(II) complexes typically have face-to-face structures with both rhodium atoms in pseudooctahedral or pseudo-square-pyramidal environments. The rhodium – rhodium bond is systematically perpendicular to the two faces, which are disposed in eclipsed or staggered conformations.[1] These characteristics are found in complexes ranging from the large family of lantern complexes with four bridging ligands $[Rh_2(\mu\text{-bridge})_4(L)_n]$ up to the cationic complex $[Rh_2(NCMe)_{10}]^{4+}$ with no bridging ligands.[1c] Analogous rhodium – rhodium bonds are even formed in complexes in which the bridging ligands prevent face-to-face structures.[1d] Here we describe unprecedented dinuclear rhodium(II) complexes with a bond between two metal atoms in coplanar square-planar environments and an unusually low electron count of 30 valence electrons.

New starting materials with bulky $PtBu_2^-$ ligands can be obtained by circumventing the inertness of known phosphido rhodium(I) complexes. In contrast to the partial replacement of 1,5-cyclooctadiene (COD) in $[\{Rh(\mu\text{-}PPh_2)_2(cod)\}_2]$ by

[*] Dr. M. A. Ciriano, Prof. L. A. Oro, Dr. C. Tejel, Dr. M. Sommovigo, Dr. J. A. López, Dr. F. J. Lahoz
Departamento de Química Inorgánica
Instituto de Ciencia de Materiales de Aragón
Universidad de Zaragoza – C.S.I.C.
50009-Zaragoza (Spain)
Fax: (+34) 976761143
E-mail: mciriano@posta.unizar.es, oro@posta.unizar.es

[**] Generous financial support from DGES (Projects PB98-641, PB95-318, and PB94-1186) and a fellowship (to M.S.) are gratefully acknowledged.